Preliminary design and validation of a single-stage Mars Ascent Vehicle

Martin Bernat
College of Engineering
Swansea University
Swansea UK
961277@swansea.ac.uk

***Abstract* - The planet Mars is often seen as a potential planet to colonize and the Mars Sample Retrieval mission aims to explore whether Mars ever supported life and to help prepare for a human exploration. This paper focuses on the single stage to orbit Mars Ascent Vehicle that would deliver the samples from the surface of Mars to its orbit to enable their delivery to Earth. Prior research suggested many options, constraints and limitations, which are explored and acted upon in this paper. Because this is a multidisciplinary project the major focus was put on the design, aerodynamics, orbiting and performance, which were improved iteratively using computational fluid dynamics in Ansys Fluent, and equations of motion and two-body problem equations implemented into a MATLAB code. Using this analysis, it was found that the final lift-off mass of the vehicle to achieve the required orbit of 580 km and 460 km is 293.143 kg. Using emerging technologies, it was proven that the performance of the vehicle can be improved compared to past proposals and with the use of more advanced computational methods and more data available, the performance could be improved even further. The proposed design would allow to deliver the samples more efficiently without the need for more complex two-stage vehicle while fulfilling all requirements.**

Keywords –Mars Ascent Vehicle, Mars exploration, Mars orbiting, Mars sample retrieval

I. INTRODUCTION

Over the years the Mars surface research has significantly contributed to the exploration and understanding of the planet. But at the current stage more emphasis needs to be put on the analysis of the Martian regolith to provide evidence and to get a deeper understanding of the evolution of the planet. Such analysis cannot be done on Mars due to the mass constraints of the payload that can be delivered on Mars and complexity of the task.

The Mars Sample Retrieval mission aims to collect and deliver samples from Mars to Earth [1]. It has a high priority in the field of space exploration because it allows the fulfilment of goals given by the Mars Exploration Program and National Academy of Sciences. These include determining if Mars ever supported life, understanding of the evolution of the climate and the geological system, and to prepare for human exploration and habitability [1], [2]. Part of this mission is the Mars Ascent Vehicle (MAV) that would deliver the samples from the surface to the orbit of Mars. The design of such a vehicle is the aim of the work detailed in this research paper. Alongside the design, the aim is to find an appropriate trajectory for the vehicle and optimize the performance using computational fluid dynamics (CFD).

Because the mission has such a high importance, many concepts have been proposed in the past. The most prominent coming from engineers and scientists from the National Aeronautics and Space Administration (NASA) in which focus was put on individual aspects of the MAV as well as implementation of them in multidisciplinary projects [3], [4], [5], [6], [7]. Because the scope of the MAV design is wide, not all the aspects will be considered in this research paper. The most important considerations for the project are the constraints and requirements. They have been changed throughout the years based on new findings and technology advances. The research described in this report is based on current requirements and technology. There are two top-level requirements, which are important for this research paper and from which all other research follows. The first requirement sets the sample cache to be a 16 cm wide sphere with a weight of 5 kg. The other one states that the orbit must have an altitude of 460 km at the periapsis and 580 km at the apoapsis with an inclination of 45° [3]. The two requirements are important for this research paper because they enable the mass estimation and optimization, which is crucial because the maximum mass is 360 kg [4].

Next the means of validating the design must be found. A number of approaches can be used to analyse the trajectory of the vehicle. In the past NASA used the Northrop Grumman Mission Capabilities Analysis Tool, modified using the Mars Geodetics and the Mars Global Reference Atmospheric Model (GRAM) to optimize the vehicle trajectory in a general design study [4]. More complex trajectory analysis performed by NASA was done in a research which used Gauss Pseudospectral Optimization Software [8]. This is a complex control software that uses the boundary, path and control constraints to enable optimization of control profiles, while allowing division of a flight into stages, making it the most efficient and accurate approach [8], [9]. In other cases, simpler optimization tools, such as 'Optimal Trajectories by Implicit Simulation program (OTIS)' and 'Program to Optimize Simulated Trajectories 3D (POST3D)', were used by NASA to find an optimum orbit

based on the lift-off mass [5]. These solutions used three degrees of freedom while solving differential equations, but they do not support any aerodynamics or propulsions models [5]. Their capabilities were enhanced using Mars GRAM in some cases [6].

The other important consideration for this project is the aerodynamic analysis. Not much research focused solely on aerodynamics has been done in the past by NASA due to changing requirements and design features. In one study, Huynh *et al.* [6] simulated both subsonic and supersonic velocities. They used engineering analysis for subsonic velocities, using CB Aero, and Euler CFD code, namely Cart3D, for supersonic velocities [6].

For the purpose of this research there were many aspects to be considered for the design as well as many approaches to take. The top-level requirements for sizing, mass and orbit altitude will have to be fulfilled. For the orbiting section of this paper, equations of motion and two-body problem equation will be used. They will be implemented into a code that solves differential equations, much like the tools OTIS and POST3D used by NASA. This will allow for a simulation and optimization of an orbit without introducing complexity of more accurate methods which are unnecessary at a preliminary stage of a design. Unlike the other tools the code produced in this paper will be enhanced by using aerodynamic data. Due to a limited aerodynamic analysis in prior research the CFD analysis in this research will be performed conventionally, using the inviscid model for subsonic speeds and viscous model for supersonic speeds.

II. FORMULATION AND METHODOLOGY

As mentioned previously the design of the MAV is a multidisciplinary project which requires deep understanding of different fields and disciplines. It is therefore impossible for a single person to be able to account for every aspect of the design process and an emphasis was put on a few fields.

The primary fields on which a major focus was placed were design, aerodynamics and orbiting and performance, which were improved through an iterative process. These fields were supported by secondary fields such as propulsion, fuel and thermal processes.

A. Requirements and constraints

The project was driven by the top-level mission requirements which were formulated by NASA and were used in other projects that focused on the design of the MAV. The simplified requirements that are relevant to this project are the following:

- To deliver a 5 kg, 16 cm wide spherical sample container to a low Mars orbit. [3]
- The achieved Mars orbit must have a periapsis greater than 460 km and an apoapsis less than 580 km with an inclination of 45° +/- 0.2° [3]
- The MAV and the igloo/erector support system must have a mass lower than 360 kg [4]

However, there is another set of constraints that could be defined as technological. These are requirements that list the existing infrastructure and technology that is available for the Mars Sample Retrieval mission (MSR). These requirements introduce constraints to the design of the MAV.

The main concern for the size limitations is the delivery of the MAV to the surface of Mars. This would be done using an aeroshell which would protect the vehicle during the landing. The standard that NASA uses is an aeroshell with the length of 4.7 meters [7]. An envelope of potential dimensions for the MAV was produced by another research and the results are shown in Table I [4]. These dimensions are the diameter of the body of the MAV and the maximum length the MAV can have for a given diameter in order to be stored. This set of data were utilized for the purposes of this project.

TABLE I
THE SIZING OPTIONS FOR THE MAV [4]

Option	MAV Diameter [mm]	MAV Maximum length [mm]
1	350	3666
2	400	3656
3	450	3630
4	500	3580
5	550	3522
6	600	3464
7	650	3410
8	700	3150

B. CAD modelling

The initial sizing followed the dimension constraints given by the technology available for delivery of the MAV to the surface of the Mars. Because the ultimate goal of the MAV is to deliver samples to an orbit of Mars the design of the vehicle revolved around the sample cache.

The first thing that needed to be considered was the placement of the sample cache. It was necessary to make sure that the storing mechanism is as simple as possible to prevent any malfunction. The majority of the research done in the past suggested placing the sample cache into the nose of the MAV [4], [7]. This effectively makes the outer surface of the cache the surface of the vehicle. As the vehicle would be placed on a platform in a horizontal orientation, the nose of the MAV would be easily accessible for a rover, which would fit the cache into the required position. This placement would be efficient for the final stages of the mission too. Previous research considered ejecting the sample cache once the vehicle reaches the required orbit to ensure simple retrieval of the cache [4]. This means that the nose is the most efficient position for the sample cache because putting the samples into the structure of the vehicle would result in logistical difficulties. The sample had to be stored safely and a mechanism that would store and hold the sample cache in its position needed to be added to the nose cone which required additional space. There are multiple solutions available for the holding mechanism. This mechanism would also jettison the cache once a desired orbit was achieved.

However, storing the cache in the nose raised concerns when it came to the ascent of the vehicle through the atmosphere. The ascent would create significant drag that would heat up the surface of the vehicle. Most

significantly at the nose where the samples were considered to be stored. Preventive measures needed to be taken to reduce the effect of heating on the sample cache. Even though the atmosphere is not as dense as in the case of the Earth atmosphere, the Mars atmosphere at the 'sea level' is only 0.02 kg/m^3 compared to 1.225 kg/m^3 of Earth [10], the risk of the samples being affected by the heat needed to be mitigated.

After a decision where to place the sample cache was made it was clear that the diameter of the vehicle and the aerodynamic properties would be derived from the size of the sample cache. The most simplistic design uses half of the spherical cache for the nose of the vehicle while the other half is inside of the vehicle where it is attached. The remaining structure of the nose is then designed to create a smooth transition. It was necessary to ensure that there was no clearance between the cache and the nose which would negatively impact the performance of the vehicle, due to the increased drag, and it would allow hot gasses to enter the internal structure.

The sizing of the remaining structure of the vehicle is based on the requirements for fuel, oxidizer and the engine. A decision needed to be made on what type of an engine should be used. In research done in the past engineers tried verifying feasibility of using solid, liquid and hybrid rocket engines for a MAV. The biggest potential lies in the hybrid rocket engines due to their performance and reliability. There is an ongoing research focused on design of an optimal hybrid engine for the MSR mission which utilizes paraffin-based fuel as a solid fuel and liquid oxygen/nitrogen as an oxidizer [7]. This combination offers great performance and survivability at low temperatures. [7]. The survivability is an important consideration because the temperatures on Mars during a night are as low as -70°C. The fuel and the oxidizer need to be protected from freezing and a requirement for a heating mechanism would only increase the complexity and the total mass. Furthermore, the hybrid engines offer a unique opportunity of gathering resources for fuel production on the surface of Mars offering a significant mass reduction [11].

Higher efficiency of the vehicle can be achieved by using multiple stages. But for the purposes of the report only a single-stage vehicle will be considered and analysed. This decision was made because to achieve good results the ideal staging concept would have to be implemented rather than the restricted staging concept. This would make the project more complex and focused on the staging, which is not its aim. Multiple stages would also introduce design complexities which are undesirable because the aim of this project is to have as simple design as possible.

As the dimensions of the structure would be determined by the volume that is needed to store a sufficient amount of fuel and oxidizer a MATLAB code that simulates the launch and trajectory of the vehicle would be utilized. This code will be explained further in section C.

The last aspect that needed to be considered were the means of controlling the ascent of the vehicle. Initially reaction control system (RCS) thrusters were considered. However, these required additional structure to be added, which made the whole system more complex, along with an addition of a fuel tank for the RCS propellant. The propellant would need to be carefully considered to make sure it could withstand low temperatures, or a heating system would need to be added which would increase the complexity even more. The simplest solution for the control of the vehicle is a nozzle that can be gimbaled. This added complexity, but it was less complex than RCS thrusters. It resulted in addition of only a small space to the structure of the vehicle for accommodation of the gimbal mechanisms. One of the interesting solutions that was discarded was the use of grind fins. Grid fins are unconventional control surfaces which consist of grids and are implemented mainly for missiles and reusable launch vehicles that require stabilization [12]. However, it was not possible to verify their performance. Because the drag is the main consideration for this project and the properties of the grid fins could not be tested in a CFD model, due to the license limitations, conventional solution of gimbal mechanisms was chosen instead.

Avionics and batteries, which are crucial for the control of the vehicle at the ground, during the ascent and orbiting, needed to be included in the planning stage of the vehicle layout. The most practical placement of the components was in the nose cone in a compartment below the payload module. Due to the lack of information on current dimensions of avionics considered for the MSR mission an assumption was made that the space in the nose cone that was left after the sample cache and the holding mechanisms were implemented was sufficient to store all the necessary systems.

C. Flight path and orbiting

To validate the capabilities and performance of the design there was a need for a development of a code that would demonstrate the success of the mission. This would be achieved by accounting for lift-off mass, fuel consumption, thrust and drag. The code was developed simultaneously with the CAD model to get a fast feedback and allow for iteration of the design. This code was created in MATLAB and its function was divided into two sections – atmospheric flight and orbiting. Each of these sections required their own set of differential equations to describe their trajectory.

For the post-launch and the atmospheric part of the flight the equations of motion were used to perform the gravity turn manoeuvre. The equations of motion are derived by resolving the Newton's second law. This yielded (1) to (4).

$$\frac{dv}{dt} = \frac{T - D - m \times g \times \sin\gamma}{m} \tag{1}$$

$$\frac{d\gamma}{dt} = -\frac{g \times \cos\gamma}{v} \tag{2}$$

$$\frac{dh}{dt} = v \times \sin\gamma \tag{3}$$

$$\frac{dx}{dt} = v \times \cos\gamma \tag{4}$$

Where v is the speed, γ is the flight path angle, h is the altitude, x is the horizontal distance travelled, T is the thrust, D is the drag, m is the mass and g is the gravitational acceleration which is a function of altitude. To avoid complexity of estimating the variation of gravitational acceleration with altitude, which is caused by anomalies [13], the variation was assumed to be identical to the one of Earth, which is described by (5):

$$g = \frac{g0}{(1 + \frac{h}{R_M})^2} \tag{5}$$

Where $g0$ is the gravitational acceleration at the sea level and R_M is the radius of Mars.

Initially, possible lift-off masses had to be estimated. This was done using the known parameters that were used to find the structural and payload ratios. The lift-off mass depends on the payload that needs to be delivered to a given orbit. The mass of the sample cache was given as 5 kg. However, another 31 kg was added to the payload mass as other projects had done before [11], [14]. This additional mass represented avionics, separation mechanism, telecommunications, thermal control systems and support structure.

The structural ratio ε depends on the available technology and the lowest possible value was desirable. As can be seen on Figure 1 and 2 the value of the structural ratio does not affect the lift-off mass, but it significantly affects the burnout velocity while the value of payload ratio λ affects both burnout velocity and the lift-off mass. The ratio ε affects the velocity because the mass remains constant and the structural mass replaces propellant that could be used to produce additional thrust.

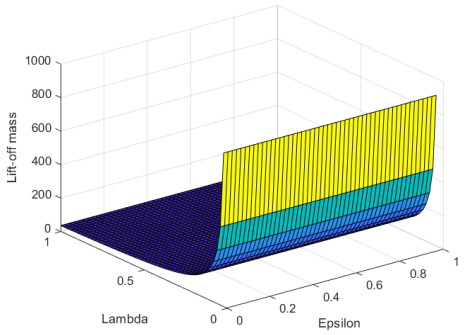

FIGURE 1
THE DEPENDENCE OF THE LIFT-OFF MASS ON THE RATIOS

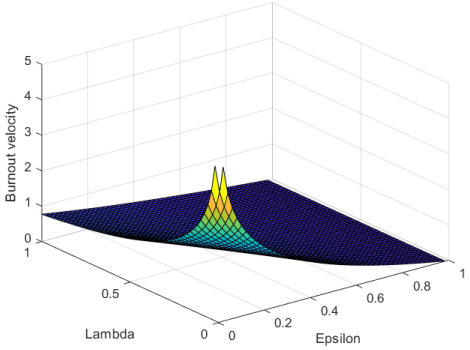

FIGURE 2
THE DEPENDENCE OF THE BURNOUT VELOCITY ON THE RATIOS

Based on previously done research a good structural ratio for a MAV is around 0.18 [11], [14]. The only unknown that remained was the payload ratio λ which can be found using (6)

$$\lambda = \frac{m_{PL}}{m_0 - m_{PL}} \tag{6}$$

where m_{PL} is the mass of the payload and m_0 is the initial mass of the vehicle.

Generally, the higher the payload ratio, the more efficient the design is. But higher payload ratio reduces the burnout velocity so a value of λ that fulfils both the mass and velocity constraints had to be found. The MATLAB code that was produced uses multiple inputs for the payload ratio with restriction to the resulting maximum mass to be lower than 360 kg. For comparison, the code also supports simulation of two-stages in which payload and the structural ratio were identical for both stages due to the restricted staging that was chosen for simplicity.

Once the lift-off masses were obtained the settings for the launch had to be set. These were based on the properties of the chosen engine and its thrust, specific impulse and the resulting mass flow rate and burn time.

As the vehicle is stored in a protective shell prior to the launch there is a need for a vertical launch to prevent any contact of the vehicle with the shell.

The trajectory that was chosen for the vehicle was one with two transfers. For the chosen engine, the velocity of the vehicle after the initial burn is too low, and the resulting trajectory cannot maintain a stable orbit. This is caused by the high thrust and high consumption of the propellant which results in a relatively short burn. This means that the engine burn has to be divided into two shorter burns rather than a single long burn. After the launch burn and a coast to an arbitrary altitude a second burn is initiated. This burn accelerates the vehicle to ensure that the apoapsis achieved is the periapsis of the final orbit that needs to be achieved – 460 km. Once the apoapsis of 460 km is reached a third burn takes place to achieve the final orbit with periapsis of 460 km and apoapsis of 580 km. A single burn, to achieve the final periapsis directly, would be more fuel efficient. But multiple burns have to be used during the ascent due to the high thrust of the engine, which is held constant in the MATLAB code, while in reality the engine should be throttled for different stages of the ascent. However, throttling is neglected in this stage of a design.

To find the total engine burn time, which is an important factor for the trajectory and launch calculations, the properties of the engine had to be considered. The thrust, specific impulse and the mass flow rate of the propellant. Using (7) and (8) the total engine burn time can be found.

$$\dot{m} = \frac{T}{ISP \times g_0} \tag{7}$$

$$t_{total\_burn} = \frac{m_p}{\dot{m}} \tag{8}$$

Where $\dot{m}$ is the mass flow rate, T is the thrust, ISP is the specific impulse, $g0$ is the standard gravity and m_p is the total mass of the propellant.

To find an optimum trajectory for the launch an ordinary differential equation solver, in this case the medium order method ode45, was used to solve the differential equations indicated in (1), (2), (3), (4). A function was created in which four different stages of the ascent are present.

- For the first five meters the launch angle is held constant so that the vehicle can leave the protective shell.
- Once the altitude is above five meters an arbitrary input is added to the derivative of the change of the flight path angle. This input allows the initiation of the gravity turn manoeuvre.
- Once the angle of π/5 rad (36 degrees) is achieved the input is removed and only the gravity will influence the flight path angle. The angle of 36 degrees was chosen based on an arbitrary input. Wide variety of inputs were manually tested, and π/5 yielded the best results.
- The last stage is for the coast. It is an unpropelled ascent which enables finding the peak of the flight path.

Once the equations have been resolved the maximum altitude of the trajectory is found. At this stage, the orbital equations needed to be used to describe the trajectory. The motion is described using the two-body problem equations of motion in an inertial frame. The motion can be described by (9) to (11):

$$\ddot{\boldsymbol{r}} = -\frac{\mu}{r^3}\boldsymbol{r} \tag{9}$$

$$\boldsymbol{r} = (X_2 - X_1)\boldsymbol{i} + (Y_2 - Y_1)\boldsymbol{j} + (Z_2 - Z_1)\boldsymbol{k} \tag{10}$$

$$r = \sqrt{(X_2 - X_1)^2 + (Y_2 - Y_1)^2 + (Z_2 - Z_1)^2} \tag{11}$$

Where μ is the standard gravitational parameter, r is the distance between the two bodies in a scalar form, $\boldsymbol{r}$ is the distance in the vector form and X_i, Y_i and Z_i, where i=1;2, are the positions of the two masses.

In the ideal case the second burn should happen at the maximum altitude to use the least propellant possible, however, because the acceleration is not instantaneous, and the burn requires constant acceleration for a specific period, the burn must happen before reaching the peak. The change in velocity, delta-v, to achieve the required periapsis is found along with the time of burn required to achieve this velocity. The actual acceleration must begin at half of the time required for the burn before reaching the peak. Even though this is the most appropriate method it resulted in different values of final apoapsis.

Because the mass before the burn was known the Tsiolkovsky rocket equation, shown in (12), could be used to find the final mass of the vehicle based on the delta-v required.

$$\Delta v = ISP \times g_0 \times \ln\left(\frac{m_0}{m_f}\right) \tag{12}$$

$$m_f = \frac{m_0}{e^{\frac{\Delta v}{ISP \times g_0}}} \tag{13}$$

This delta-v would change from the ideal value because the acceleration is not instantaneous, but an assumption was made that the ideal delta-v would be used to find the final mass to simplify the calculations. The reason why this assumption could be made is because the change in the delta-v is not significant.

The burn time to achieve a given delta-v can then be found using the initial (m_0) and final (m_f) masses and the mass flow rate of the propellant and is shown in (14).

$$t_{burn} = \frac{m_0 - m_f}{\dot{m}} \tag{14}$$

The change in delta-v required for the Hohmann transfer was found using the equations of conservation of momentum indicated as (15), (16) and (17).

$$h_m = \sqrt{2\mu\frac{r_1 \times r_2}{r_1 + r_2}} \tag{15}$$

$$v_i = \frac{h_m}{r_i} \tag{16}$$

$$\Delta v = v_2 - v_1 \tag{17}$$

Where h_m is a momentum, v_i, where i=1;2, are speeds at any two orbits and r_i, where i=1;2, are the radii of any two orbits.

There was a need to find a more accurate delta-v for the transfer to ensure reaching the designated orbit. This was done using an iterative process. This iterative process uses the current and the final velocity of the vehicle to find the apoapsis. By incrementally increasing the value of the final velocity, and running the ordinary differential equation solver, the final apoapsis increases until the desired orbit is achieved. The resulting delta-v is then used in the final version of the calculation. The same process is used for the third burn.

At the end of the code all the data is collected into a single variable, plotted and analysed. The loop then repeats with a different payload ratio. The payload ratio that enables the smallest lift-off mass needs to be used. However, it needs to fulfil the two basic conditions. Have mass less than 360 kg and have enough fuel to reach the orbit.

D. Computational fluid dynamics simulations

The main goal of the computational fluid dynamics (CFD) analysis was to validate the aerodynamics of the vehicle and to eliminate any potential flaws in the design. The main output was the coefficient of drag of the vehicle, which allows the calculation of more accurate results in the trajectory analysis using the MATLAB code. The analysis was performed using ANSYS Fluent. The analysis was intended to be run at different altitudes and velocities to validate the performance at different stages

of the flight. However, due to complexity of analysis at hypersonic speeds and the limitations for a student version of the software, only the subsonic results can be considered reliable.

The first step was preparing the model and the domain for the simulation. Whenever the design was changed a model created in SolidWorks was exported as a .STEP file and imported into the DesignModeler tool. In this tool the flow domain was created. The domain was divided into two sections with a wider area and the immediate surroundings of the vehicle. The body mesh was created using the wider domain and the body of influence type mesh. In this case the body of influence was the surroundings of the vehicle. The face mesh was created using the element size type mesh. The size of the elements was the same for both face and body mesh. Lastly the inflation layer was applied to ensure smooth transition between the faces of the vehicle and the flow domain. This is particularly important for the type of analysis that is required for this project. Because to find the most accurate coefficient of drag the mesh at the faces of the vehicle must be as fine as possible. However, the maximum number of elements for a student version of the software is limited to 512 000. This enables only a limited accuracy of the results. Nonetheless, two convergence studies were performed.

The first convergence study focused on the sizing of the mesh itself. There were many inputs that could be varied but the one that was chosen was the body element size. The size was refined until the maximum number of elements was reached which occurred when the maximum size of an element was 0.046 meters. The change to the previous results was 2.4 % which indicates that even though the results did not converge the error will not be that high. Simultaneously the other convergence study was performed which focused on variation of the domain width. The element limitation lead to the width of the domain of 5 meters with a difference to a previous size of 1.75 %. Both convergence studies are shown in a Figure 3.

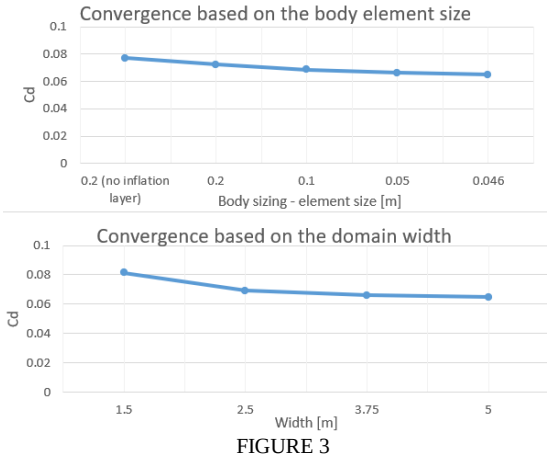

FIGURE 3
THE CONVERGENCE STUDIES FOR THE MESH

A tetrahedral mesh was set based on the results of the convergence studies. The size of the elements was constant for faces and the body and was set to 0.046 meters with a growth rate for the body of 1.116. As the flow around the surface of the vehicle was the most important 15 inflation layers with the growth rate of 1.2 were added to improve the mesh. The values of the settings of the mesh can be seen in Table II.

TABLE II
THE INFORMATION ABOUT THE MAV, REQUIREMENTS AND THE RESULTS

Body Sizing Element size [m]	0.046
Body Element Growth rate	1.116
Face Sizing Element size [m]	0.046
Inflation - max layers	15
Inflation transition ratio	0.272
Domain width [m]	5
Domain height [m]	8
Domain depth [m]	2.5
Nodes	107539
Elements	508181

The last stage was the setup of the simulation. The models that were considered in the simulations were the energy equation, which is important for higher velocities, and the Spalart-Allmaras viscous model. The Spalart-Allmaras is a simple, single equation model which yields good results for close surface flow which allows to produce accurate results for drag which is ideal for the purpose of this analysis.

Next the fluid properties needed to be set up. To obtain the necessary information the MATLAB code would be used to obtain the components of velocity, altitude, pressure (p), density (ρ) and temperature. This set of data, along with the assumption that the Martian air is an ideal gas, and other required properties such as viscosity and molecular weight were used as an input.

The required properties could be calculated using (18), (19) and (20) by using the altitude h: [15]

$$Temperature = -23.4 - 0.00222 \times h \tag{18}$$

$$p = 0.699 \times e^{-0.00009 \times h} \tag{19}$$

$$\rho = \frac{p}{0.1921 \times (T + 273.1)} \tag{20}$$

To find the speed of sound c and the Mach number M of the flow, (21) and (22) were used.

$$c = \sqrt{\gamma \times R \times T} \tag{21}$$

$$M = \frac{v}{c} \tag{22}$$

The simulations were then run for an arbitrary number of iterations until the results converged.

III. RESULTS

The atmosphere and conditions on Mars turned out to be a challenge for the launch. One difficulty that was encountered was the gravity turn manoeuvre which was performed at the beginning of the mission. Due to the significantly lower gravitational acceleration, than the one encountered on Earth, the manual input to the flight path angle had to be much more significant than it would be in

the case of Earth. The input that was chosen was a change of 0.08 radians per second after the vehicle had left the protective shell until the angle of 36 degrees was reached after which the gravity was the only thing that influenced the flight path angle.

Another aspect was the engine burn time, specifically the launch burn time. It was not known what the altitude or velocity that should be reached after the first burn was, nor what the optimum settings are for the most fuel-efficient ascent. Multiple settings were tested, and the decision was made that the most efficient results were obtained when the engine was using 45 % of the total burn time of the engine for the launch burn.

As all these selections were arbitrary options, the results that were obtained might not be the optimal for the tested values.

Several settings were tested using the MATLAB code and the results of the most suitable setup are shown in the following sections of this project.

A. *Mission sequence*

Using (7) and (8) the total burn time was found to be 94.2 seconds. Based on prior research the thrust used was 7464 N [14] and specific impulse was 338 s [16]. The engine burn time for the launch was set at 45 % of the total engine burn time resulting in 42.4 second burn after which the vehicle reached the altitude of 11.6 km at a velocity of 1.082 km/s and flight path angle of 27.6 degrees. At this stage the vehicle starts to coast until it reaches the apoapsis of its orbit at the altitude of 43.9 km and the velocity of 0.848 km/s which are achieved at 179.8 seconds into the flight.

However, the apoapsis data were not important because as mentioned in the methodology section of this project, the next burn had to start before reaching the apoapsis. Using the Tsiolkovsky rocket equation, shown in (12), the final mass after the burn was found using the required delta-v along with the time required to achieve this speed which was found using (14).

The second burn was found to be 50.1 seconds. This meant that the burn had to be started 25.05 seconds before reaching the apoapsis. This changed the delta-v required for the transfer and the actual value had to be found through iterations rather than using the equations of conservation of momentum. The delta-v was found to be 2.7586 km/s. The same approach was taken for the third – final burn. The burn was significantly shorter than the previous two and required only 1.65 seconds which resulted in the delta-v of 0.1496 km/s.

The results of this analysis are shown in Table III. They indicate that the final lift-off mass for the vehicle is 293.143 kg.

The final trajectory can be seen in Figure 5 and the whole mission with the individual manoeuvres is shown in Figure 4. It shows the variation of the speed and the altitude in the scope of the initial 3000 seconds. The variation of velocity in the graph is particularly important because it shows significance of the individual engine burns and their effect on the speed and increase in altitude.

TABLE III
THE INFORMATION ABOUT THE MAV, REQUIREMENTS AND THE RESULTS

Take-off mass [kg]	293.143
Dry mass [kg]	82.286
Propellant mass [kg]	210.857
Leftover propellant [%]	0.080
Apoapsis altitude [km]	579.908
Periapsis altitude [km]	459.946
delta-v1 [km/s]	2.7586
delta-v2 [km/s]	0.1496

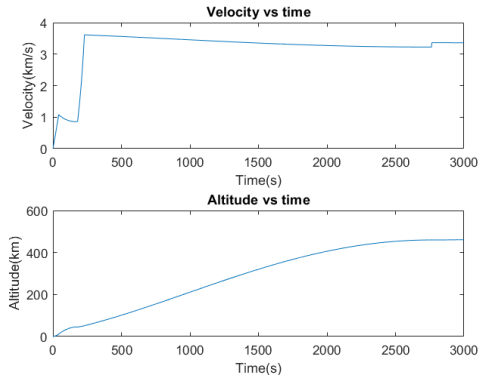

FIGURE 4
THE VARIATION OF ALTITUDE AND VELOCITY FOR THE MISSION

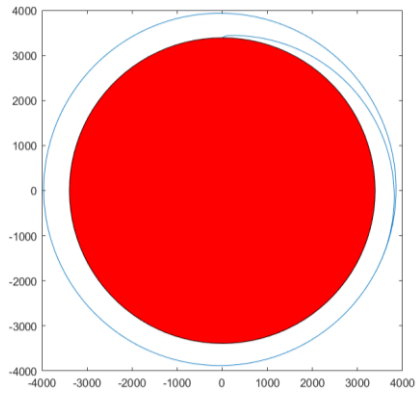
FIGURE 5
THE FINAL TRAJECTORY OF THE VEHICLE WITH DISTANCES IN KM

B. *The final design of the MAV*

To achieve the required performance the diameter of the vehicle was reduced to 0.35 meters to decrease the frontal area which resulted in a decrease of drag. This diameter along with the diameter of the sample cache, which is 0.16 meters, dictated the shape of the nose cone of the vehicle which was one of the main design considerations for the mission. These constraints did not allow much flexibility and caused that the nose of the vehicle is blunt. The biggest challenge was to make the transition between the sample cache and the nose cone structure as smooth as possible not to cause additional drag. However, this was only possible to a certain level.

The size of the body of the vehicle was chosen based on the propellant requirements. The propellant mass, found using the MATLAB code, was found to be 210.857 kg. Because the hybrid rocket engine was used, this mass needed to be split between the oxidizer and the fuel which had to be stored separately. An important consideration was the ratio of the oxidizer to the fuel, known as the O/F ratio, required for the best engine

performance. Based on the research done in the past the best performance and therefore highest specific impulse of an engine can be achieved by using the O/F ratio of values between 2 and 3 [14], [16]. For the purposes of this project the value of the O/F ratio, based on the stoichiometric ratio, was assumed to be 2.2. This resulted in the mass of the fuel being 65.893 kg and the oxidizer mass 144.964 kg. To find out the volume required to store these, their density needed to be found. The average density of liquid oxygen oxidizer is 1141 kg/m^3 and the density of the paraffin wax is 900 kg/m^3. This meant that the volume required was 0.0732 m^3 for the fuel and 0.12701 m^3 for the oxidizer. The storage tanks were assumed to have the internal diameter of 0.31 meters and were assumed to have a cylindrical shape, which is not an ideal shape for storage of pressurized gasses or liquids but was used as a simplified model. Using these assumptions, the height of the tanks was found to be 0.97 meters for the fuel and 1.683 meters for the oxidizer. This meant that the height of the body had to be higher than 2.653 meters. Additional space needed to be included for valves and the engine. The resulting height of the body was set to 2.91 meters. The final layout of the vehicle with the internal structure can be seen in Figure 6.

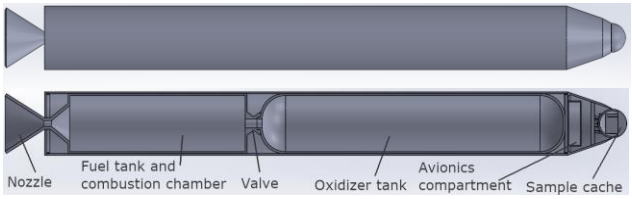

FIGURE 6
THE EXTERNAL AND INTERNAL STRUCTURE OF THE MAV

C. *Aerodynamic analysis*

The aerodynamic analysis was considered once the general dimensions of the vehicle were decided. The restrictions of the software that was available had a significant impact on the analysis. The number of surfaces were limited so the general design had to be made as simple as possible to allow for the most accurate results. Another constraint was the mesh which was limited to 512 000 elements. So even though the convergence study had been done the results could not be taken as the most accurate. Nevertheless, they could be considered viable for the purposes of a preliminary design.

The first thing that was created was the flow domain. The sizing of the domain was decided based on the convergence studies that was done in the methodology section and the resulting domain with the final design of the vehicle is shown in Figure 7.

The analysis needed to be considered at different stages of the flight. The inputs, such as the pressure, temperature, density and speed of sound, for the simulations were found based on the altitude, velocity and the properties of the Martian air. The properties that needed to be utilized were the heat capacity ratio γ, which is 1.3, and the gas constant R which is equal to 192 J/kg.K [17]. The values that were found are shown in the Table IV.

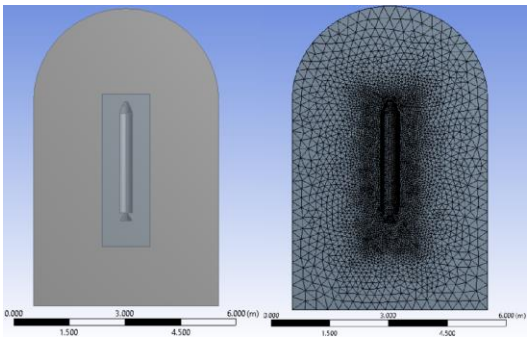

FIGURE 7
THE FLOW DOMAIN AND THE MESH USED FOR THE ANALYSIS

TABLE IV
THE INPUTS FOR THE CFD ANALYSIS FOR INDIVIDUAL SIMULATIONS

Test number	1	2	3	4
Time [s]	3.5	9.3	33.4	42.2
v [m/s]	86.2	259.5	840.4	1082.3
h [m]	146.6	1042.6	7605.4	11633.4
T [K]	249.4	247.4	234.6	230.5
c [m/s]	249.5	248.5	242.0	239.9
M	0.35	1.04	3.47	4.51
p [kPa]	0.690	0.636	0.353	0.245
rho [kg/m^3]	0.014	0.013	0.008	0.006

These values were used as an input for the analysis for four different stages of the flight.

The first stage that was analysed took place shortly after the launch at subsonic, incompressible conditions. Figure 8 shows the velocity and pressure distribution around the vehicle which indicate no complications or irregularities during this stage.

The second stage that was analysed took place at the transonic stage of the flight. This stage is shown in Figure 9. There is a significant pressure increase at the tip of the vehicle caused by a normal shock. At the bottom of the nose cone the pressure significantly decreases and velocity increases which is caused by an expansion fan.

The third stage that was analysed took place at hypersonic velocity. This stage is shown in Figure 10 which shows a shock cone generated by the normal shock.

The last stage that was analysed took place at the maximum dynamic pressure, which occurred at Mach 4.5, 42.2 seconds into the flight which was at the end of the launch burn. This fact was found using the MATLAB code which was used to create a plot of a dynamic pressure variation with time. This is shown in Figure 11.

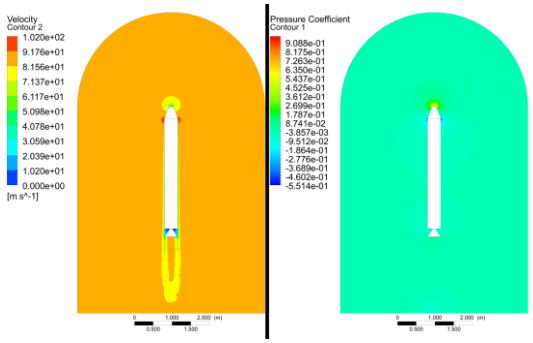

FIGURE 8
THE COEFFICIENT OF PRESSURE DISTRIBUTION (ON THE RIGHT) AND THE VELOCITY DISTRIBUTION (ON THE LEFT) FOR STAGE 1 (MACH 0.3)

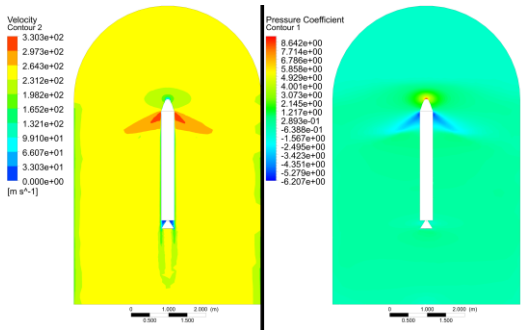

FIGURE 9

THE COEFFICIENT OF PRESSURE DISTRIBUTION (ON THE RIGHT) AND THE VELOCITY DISTRIBUTION (ON THE LEFT) FOR STAGE 2 (MACH 1)

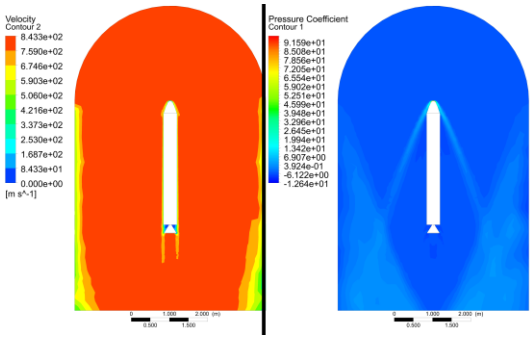

FIGURE 10

THE COEFFICIENT OF PRESSURE DISTRIBUTION (ON THE RIGHT) AND THE VELOCITY DISTRIBUTION (ON THE LEFT) FOR STAGE 3 (MACH 3.5)

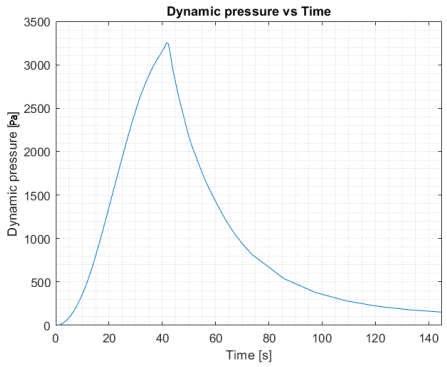

FIGURE 11

DYNAMIC PRESSURE DISTRIBUTION FOR THE LAUNCH

The resulting coefficients of drag (Cd), drag (D) and dynamic pressure (q) are shown in Table V. These results created the basis for an input to the MATLAB code which allowed to adjust the lift-off mass. Due to the complexity required for the CFD simulations the coefficient of drag distribution between the tested stages was assumed linear, which creates an error compared to an exponential distribution it should have. The implementation to the MATLAB code was done by assigning a coefficient of drag based on the velocity of the vehicle. The altitude did not change the coefficient of drag because the simulations were run under the same conditions at the real altitudes the vehicle would have so the velocity became the only variable.

TABLE V

RESULTING COEFFICIENTS OF DRAG WITH THE FINAL DRAG

q [Pa]	53.5	450.6	2763.0	3244.5
Cd	0.085	0.944	5.974	7.092
D [N]	0.4	41.0	1806.5	2519.1

IV. DISCUSSION

A. *The final design*

As there were multiple disciplines utilized side by side there were many obstacles in the design of the vehicle. Due to lack of information and data available to public, the focus of the design was put on fulfilling the known top level and technological requirements.

The implementation of the design was made as simple as possible not to introduce additional challenges not only for other design stages but also for the flight and pre-flight of the vehicle. The design choices that were made had a positive impact on the mission. By choosing the minimum diameter of the aircraft possible, the frontal area of the vehicle is reduced resulting in lower drag. This selection does not jeopardize other parts of the design. It was necessary to increase the length of the vehicle to store enough propellant to fulfil the orbit requirements but the maximum length of 3666 millimetres indicated in Table I, which is necessary to be able to store the vehicle and deliver it to the Mars surface, was achieved.

In the future research the focus must be put on the smaller but not less significant parts of the design such as the avionics, RCS thrusters or the engine itself whose analysis was limited to a minimum in this research project due to the time constraints. Nonetheless, the design of the vehicle is similar to what other projects proposed in the past such as the design proposed by Northrop Grumman Aerospace Systems [4]. The design is proposed as a single stage solution but there are no limitations for the use in a two-stage solution in which case the aerodynamics of the vehicle would not change much and the only reason why they would, is the change in the length of the vehicle.

B. *The aerodynamics of the final design*

The limited aerodynamic analysis that was performed helped improve the design of the vehicle by providing more accurate data for drag. Only a limited amount of aerodynamic analysis for a MAV are available to the public so there was no data to compare the results of the CFD analysis to.

The results of the CFD analysis cannot be deemed accurate for compressible flow which makes up majority of the mission. This is caused by the limitations of the software used and the fact that at hypersonic speeds the data should be validated by wind tunnel testing.

Because the density of the Mars atmosphere is very thin the drag that was found at all stages of the flight does not affect the mission significantly. By choosing the launch burn time as 45 % of the total burn time the maximum dynamic pressure occurs at the end of this burn and has a value of 2519.1 Newtons which is comfortably counteracted by the thrust. The maximum dynamic pressure has a value of 3244.5 Pa which is lower than a maximum dynamic pressure for another research in which it was expected to be 6000 Pa [8]. If the burn had been longer the effects of the drag would grow stronger and could increase the amount of fuel required.

This analysis was affected by a limited time so in the future it is necessary to perform more in-depth optimization of the design features of the vehicle.

C. The trajectory and orbit of the mission

The trajectory and orbit optimization were affected by many arbitrary inputs and assumptions. The arbitrary inputs were varied and tested to get the best performance, however, this means that the solutions that were found might not be the best available and in the future more focus should be put in their optimisation.

Nevertheless, the results that were obtained using the MATLAB analysis were promising. The total lift-off mass was found to be 293.143 kg with only 0.08% of fuel left and the final orbits are only 100 meters off the target values. These results fulfil all the requirements.

The lift-off masses of MAVs that were designed in the past are close to the value of the lift-off mass found in this project. For a single-stage vehicles the lift-off masses were: 326.69 kg [4] and 374.3 kg [11] and for two-stage vehicles: 223.9 kg [11], 248.4 kg [14], 250.95 kg [4]. The mass found in this research is close to the two-stage vehicles. This is caused by the many assumptions that were made as well as improving technology because many of these projects were done in the early 2010s. This indicates that the design of the vehicle was improved compared to others and is feasible for the mission.

V. CONCLUSION

This research project conducted an investigation of the preliminary design of a single-stage Mars Ascent Vehicle based on the research that had been done in the past and the new technologies that emerged.

A design of the vehicle was proposed that fulfils the mission and technological requirements. This design incorporates a liquid oxygen/paraffin hybrid engine whose high efficiency enables significant lift-off mass reduction. An aerodynamic analysis in ANSYS Fluent was performed at different stages of the flight to optimize the design and to find coefficients of drag to allow for optimization of the launch and orbiting. A flexible MATLAB code was developed which allows to find lift-off masses based on variable payload ratio which enables to iteratively improve the flight. The coefficients of drag found in the aerodynamic analysis are implemented in the code which enables accurate estimation of the fuel consumption during the launch stage of the mission.

The final lift-off mass that was found is 293.143 kg which is 33 kg less than another research suggested [4]. The selected design meets the technological requirements for delivery and the survival on the Mars surface. The trajectory and orbiting section of this project verifies that the vehicle can deliver the sample cache to the required orbit with an accuracy of 100 meters. With further research focused on the secondary aspects of the design, more accurate and advanced computational methods and more data that is currently classified for the public, the design of the vehicle could become a feasible option for the Mars Sample Retrieval mission and help the humanity benefit from the greatest scientific feat ever conducted.

VI. ACKNOWLEDGEMENT

The author would like to thank Dr Nick Croft for the support and guidance throughout the project.

VII. REFERENCES

[1] Committee on planetary science decadal survey, Advancing Studies of Mars, In: National Research Council of the national academies. Vision and Voyages for Planetary Science in the Decade 2013-2022. Washington DC: The National Academies Press; 2011. p. 164.

[2] Banfield D, Johnson S. S, Stern J, Brain D, Withers P, Wordsworth R, et al. Mars Science Goals, Objectives, Investigations, and Priorities: 2018 Version. 2018 Version ed. [Cornell University]: Mars Exploration Program Analysis Group (MEPAG); 2018.

[3] Anderson DJ, Glaab L, Munk MM, Pencil E, Dankanich J, Peterson T. Status of Sample Return Propulsion technology development under NASA's ISPT program. NASA Center for AeroSpace Information (CASI). 2012. [4 p.]

[4] Trinidad MA, Zabrensky E, Sengupta A. Mars Ascent Vehicle system studies and baseline conceptual design. 2012 IEEE Aerospace Conference. 2012.

[5] Dux IJ, Huwaldt JA, Dankanich JW, McKamey RS. Mars Ascent Vehicle Gross Lift-off Mass Sensitivities for Robotic Mars Sample Return. 2011 Aerospace Conference. 2011.

[6] Huynh LC, Jiang XJ, Hawke VM, Bowles JV. Mars Sample Return: Mars Ascent Vehicle Mission and Technology Requirements. NASA Center for AeroSpace Information (CASI). 2013.

[7] Shotwell R, Benito J, Karp A, Dankanich J. A Mars Ascent Vehicle for potential mars sample return. 2017 IEEE Aerospace Conference. 2017

[8] Benito J, Shotwell R. Trajectory design for a Mars Ascent Vehicle concept terrestrial demonstration. 2017 IEEE Aerospace Conference. 2017.

[9] Agamawi Y, Rao A. CGPOPS: A C++ Software for Solving Multiple-Phase Optimal Control Problems Using Adaptive Gaussian Quadrature Collocation and Sparse Nonlinear Programming. University of Florida, Gainesville, 2019.

[10] Williams DR. NASA Mars fact sheet [Internet]. [Greenbelt]. NASA Space Science Data Coordinated Archive (NSSDCA). [date unknown]. [updated 2018 Sep 27; cited 2020 Apr 14]. Available from: https://nssdc.gsfc.nasa.gov/planetary/factsheet/marsfact.html

[11] Boiron AJ, Cantwell BJ, Hybrid Rocket Propulsion and In-Situ Propellant Production for Future Mars Missions. 49th AIAA/ASME/SAE/ASEE Joint Propulsion Conference. 2013

[12] Peng K, Hu F, Wang D, Okolo PN, Xiang M, Bennett GJ, et al. Grid fins shape design of a launch vehicle based on sequential approximation optimization. Advances in Space Research. 2018

[13] Neumann GA, Zuber MT, Wieczorek MA, McGovern PJ, Lemoine FG, Smith DE. Crustal structure of Mars from gravity and topography. Journal of Geophysical Research: Planets. 2004;109(E8)

[14] Chandler AA, Cantwell BJ, Scott Hubbard G, Karabeyoglu A. Feasibility of a single port Hybrid Propulsion system for a Mars Ascent Vehicle. Acta Astronautica. 2011;69(11-12):1066-72.

[15] National Aeronautics and Space Administration [Internet]. [Cleveland]: Glenn research center; [date unknown] Mars Atmosphere model; [cited 2020 Apr 14]; Available from: https://www.grc.nasa.gov/WWW/K-12/airplane/atmosmrm.html

[16] Karabeyoglu A, Stevens J, Geyzel D, Cantwell D. High Performance Hybrid Upper Stage Motor. 47th AIAA/ASME/SAE/ASEE Joint Propulsion Conference. 2011

[17] Mars physical and orbital statistics, comparisons. [Internet], [Ames], Iowa State University Department of Geological and Atmospheric Sciences. [date unknown]. [updated 2012 Nov 06; cited 2020 Apr 14]. Available from: https://meteor.geol.iastate.edu/classes/mt452/Class_Discussion/Mars-physical_and_orbital_statistics.pdf